THE UNIVERSITY *of* EDINBURGH

Edinburgh Research Explorer

Quantitative analysis of regulatory flexibility under changing environmental conditions

OPEN ACCESS

molecular
systems
biology

Quantitative analysis of regulatory flexibility under changing environmental conditions

Kieron D Edwards[1,6], Ozgur E Akman[2,7], Kirsten Knox[1], Peter J Lumsden[3], Adrian W Thomson[1], Paul E Brown[4], Alexandra Pokhilko[1], Laszlo Kozma-Bognar[5], Ferenc Nagy[1,5], David A Rand[4] and Andrew J Millar[1,2,*]

[1] School of Biological Sciences, University of Edinburgh, Edinburgh, UK, [2] Centre for Systems Biology at Edinburgh, Edinburgh, UK, [3] University of Central Lancashire, Preston, Lancashire, UK, [4] Warwick Systems Biology Centre, University of Warwick, Coventry, UK and [5] Biological Research Centre of the Hungarian Academy of Sciences, Szeged, Hungary
[6] Present address: Advanced Technologies (Cambridge) Ltd, Cambridge, UK
[7] Present address: College of Engineering, Mathematics & Physical Sciences, University of Exeter, Exeter, UK
* Corresponding author. Centre for Systems Biology at Edinburgh, University of Edinburgh, C. H. Waddington Building, Kings Buildings, Edinburgh EH9 3JD, UK.
Tel.: + 44 131 651 3325; Fax: + 44 131 650 5392; E-mail: andrew.millar@ed.ac.uk

The circadian clock controls 24-h rhythms in many biological processes, allowing appropriate timing of biological rhythms relative to dawn and dusk. Known clock circuits include multiple, interlocked feedback loops. Theory suggested that multiple loops contribute the flexibility for molecular rhythms to track multiple phases of the external cycle. Clear dawn- and dusk-tracking rhythms illustrate the flexibility of timing in *Ipomoea nil*. Molecular clock components in *Arabidopsis thaliana* showed complex, photoperiod-dependent regulation, which was analysed by comparison with three contrasting models. A simple, quantitative measure, Dusk Sensitivity, was introduced to compare the behaviour of clock models with varying loop complexity. Evening-expressed clock genes showed photoperiod-dependent dusk sensitivity, as predicted by the three-loop model, whereas the one- and two-loop models tracked dawn and dusk, respectively. Output genes for starch degradation achieved dusk-tracking expression through light regulation, rather than a dusk-tracking rhythm. Model analysis predicted which biochemical processes could be manipulated to extend dusk tracking. Our results reveal how an operating principle of biological regulators applies specifically to the plant circadian clock.
Molecular Systems Biology **6**: 424; published online 2 November 2010; doi:10.1038/msb.2010.81
Subject Categories: metabolic and regulatory networks; plant biology
Keywords: Arabidopsis thaliana; biological clocks; dynamical systems; gene regulatory networks; mathematical models; photoperiodism

Introduction

Most eukaryotes and some prokaryotes possess circadian clocks, which regulate ∼24 h rhythms in metabolism, physiology and behaviour, allowing organisms to anticipate predictable changes in the day/night cycle (Bell-Pedersen *et al*, 2005). All known circadian clock mechanisms comprise surprisingly complex circuits of nested or interlocked feedback loops (Bell-Pedersen *et al*, 2005; Kitayama *et al*, 2008). Microarray studies in organisms from mammals (Panda *et al*, 2002; Ueda *et al*, 2002) to plants (Edwards *et al*, 2006; Covington *et al*, 2008; Michael *et al*, 2008) have shown that large numbers of genes are rhythmically expressed, and that functionally related genes are often co-regulated at specific times of the day. Light and temperature signals entrain the clock mechanism to set the circadian phase, which describes

the timing of endogenous rhythms relative to the environmental cycle (Bell-Pedersen *et al*, 2005). Normal circadian timing benefits growth and survival (Ouyang *et al*, 1998; Dodd *et al*, 2005), most probably due to the regulation of biological processes to an optimum phase in the daily cycle.

Coordinating biochemical activity with the timing of dusk and dawn could provide a particular benefit in the case of carbon metabolism (Dodd *et al*, 2005). Some of the carbon fixed by photosynthesis is stored in the chloroplasts as transitory starch, which is broken down to provide a source of sugars throughout the night, preventing starvation-induced inhibition of plant growth (Zeeman *et al*, 2007; Graf *et al*, 2010). Several genes involved in starch metabolism are rhythmically regulated (Harmer *et al*, 2000; Smith *et al*, 2004; Blasing *et al*, 2005; Edwards *et al*, 2006; Michael *et al*, 2008). Their expression profiles over a light/dark cycle

combine circadian control, direct regulation by light and indirect light regulation by sugar signalling and by circadian entrainment (Blasing *et al*, 2005; Usadel *et al*, 2008). Systems biology aims to support quantitative analysis, understanding and intervention in such complex, dynamic systems.

In temperate regions, the length of the day (photoperiod) changes markedly with the seasons. Many organisms use a photoperiod signal to time annual transitions in development, such as flowering or bud dormancy in plants and reproductive development in mammals and birds (Dunlap *et al*, 2004). The circadian clock underlies the measurement of day length for these important annual events (Bohlenius *et al*, 2006; Imaizumi and Kay, 2006; Hazlerigg and Loudon, 2008). Our focus here is on the timing of biological processes within the day/night cycle, rather than on the amount of a photoperiod-dependent response. The timing of circadian rhythms might be expected to respond to a changing photoperiod, in order to anticipate a particular phase of the day/night cycle robustly under many conditions. Consistent with this notion, the phase of particular circadian rhythms in plants has been shown to alter with the photoperiod (Millar and Kay, 1996; Love *et al*, 2004; Perales and Mas, 2007).

If multiple phases of the day/night cycle have adaptive significance, then an important question is how biological rhythms gain the flexibility to track each of the external phases, most obviously dawn and dusk, as their relative timing changes with the seasons. We previously used mathematical analysis to understand the design principles that might underlie the complex, interlocking feedback loop circuits that have been identified in all circadian clock mechanisms. Tunability of period under constant conditions has been proposed as one benefit from mixed feedback circuits (Tsai *et al*, 2008). Environmental noise was shown to favour loop complexity in clock systems evolved *in silico* to anticipate environmental transitions (Troein *et al*, 2009). Our analytical results showed that the presence of multiple negative feedback loops could increase the flexibility of a clock gene network, for example, permitting distinct regulation of multiple phases in light/dark cycles (Rand *et al*, 2004, 2006). We have recently shown that such flexibility can support increased robustness, as defined by Kitano (2007), if the flexibility is appropriately linked to environmental changes (Akman *et al*, 2010).

The clock gene network of the model plant *Arabidopsis thaliana* is based on a feedback loop involving two closely related transcription factors, *CIRCADIAN CLOCK ASSOCIATED 1* (*CCA1*) and *LATE ELONGATED HYPOCOTYL* (*LHY*), and the pseudo-response regulator *TIMING OF CAB EXPRESSION 1* (*TOC1*) (McClung, 2006). Understanding of the plant clock has been formalised progressively in mathematical models (Supplementary Figure 1; Locke *et al*, 2005a, b, 2006; Zeilinger *et al*, 2006). An initial model consisted of a single loop, in which a combined CCA1 and LHY protein repressed the expression of *TOC1*, which in turn induced the expression of *CCA1/LHY* (Locke *et al*, 2005a). Inability of this model to explain the experimental data in clock mutants led to its extension to include an interlocked, evening feedback loop between *TOC1* and a hypothetical gene *Y*, and a morning feedback loop between *LHY/CCA1* and the combined *TOC1* paralogues *PSEUDO-RESPONSE REGULATOR 7* (*PRR7*) and *PRR9* (Locke *et al*, 2005b, 2006; Zeilinger *et al*, 2006). The model is highly

light responsive: light signals activate transcription of *LHY/CCA1*, *PRR7/9* and *GI* genes and degradation of TOC1 protein. Model predictions and experimental evidence led to the proposal of *GIGANTEA* (*GI*) as a candidate for part of the *Y* function in the evening loop (Locke *et al*, 2006), and recent data confirm that *GI* alone does not account for *Y* function (Martin-Tryon *et al*, 2007; Ito *et al*, 2009). Additional gene-regulatory loops (McWatters *et al*, 2000; Hazen *et al*, 2005; Pruneda-Paz *et al*, 2009) and cytosolic signalling mechanisms (Dodd *et al*, 2007) have yet to be included in the models, and these may contribute further complexity to the plant clock.

The existence of coupled feedback loops in the plant clock opens the possibility for increased flexibility in the relative phase of clock components (Locke *et al*, 2006). This is analogous to the coupled 'evening' (E) and 'morning' (M) oscillators that allow the activity rhythms of nocturnal rodents to track the predicted times of dusk and dawn, respectively (Pittendrigh and Daan, 1976). Distinct groups of neurones exhibit E and M properties in *Drosophila* and in the mouse, with strong, intercellular coupling to combine their properties in the intact animals (Jagota *et al*, 2000; Stoleru *et al*, 2004; Inagaki *et al*, 2007). Plant cell clocks, in contrast, are only weakly coupled by circadian signals within each organ (Thain *et al*, 2000; Fukuda *et al*, 2007), although light signals can indirectly couple clocks in distant organs (James *et al*, 2008). Our understanding of the plant clock mechanism emphasises intracellular regulation, because it is based upon data for genes that are broadly expressed within aerial plant tissues. Tissue- and organ-specific modifications of the plant clock mechanism may provide an additional level of complexity to spatially distinct rhythms (Thain *et al*, 2002; Para *et al*, 2007).

In this study, we combined experimental and theoretical approaches to determine how much the potential flexibility of the three-loop circuit has been exploited in the evolution of the actual circadian system in Arabidopsis seedlings. Expression profiles for the Arabidopsis clock genes were measured across multiple photoperiods, with new controls for the *LUCIFERASE* (*LUC*) reporter gene imaging methods. 'Dusk sensitivity' is introduced as a simple measure for the pattern of entrainment of any circadian rhythm, and is applied to reveal the distinct regulation characteristic to each of the Arabidopsis clock models. The *in vivo* data validated the structure and detailed behaviour of the evening loop in the three-loop clock model, and quantified the behaviour of morning genes for future models. Finally, the dusk sensitivity measure was extended to predict how the entrainment of a three-loop clock could be manipulated to extend dusk tracking.

Results

Contrasting entrainment patterns in a model species for classical plant physiology

'Short-day' plants such as *Ipomoea nil* (*Pharbitis nil*) trigger flowering under shortening day lengths (with correspondingly lengthening nights). Such species have long been known for 'dusk-tracking' entrainment (Heide *et al*, 1988; Thomas and Vince-Prue, 1997). Plants of *I. nil* grown in constant light were not induced to flower (as in light:dark cycles with a long photoperiod), until they were transferred to a test interval of
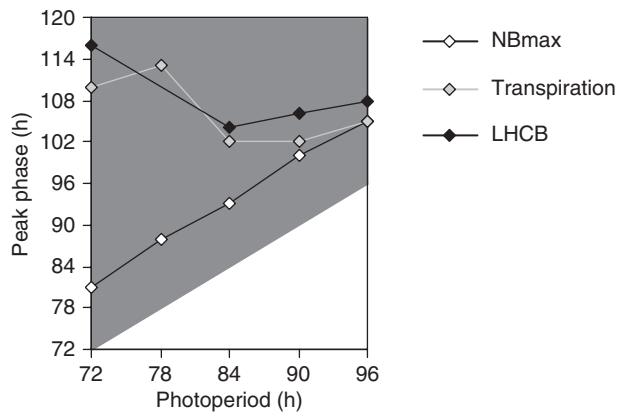
Figure 1 Dawn- and dusk-dominant rhythms show flexible timing in *Ipomoea nil*. Peak times are shown for rhythms of *LHCB* expression (filled symbols), transpiration rate (shaded symbols) and maximum inhibition of flowering by a red light pulse (NBmax, open symbols), measured in darkness after different light intervals in *I. nil*. Shaded area of plot, darkness; open area, light.

constant darkness that mimicked a long night. The circadian rhythm that controls flowering was measured by the repression of flowering in response to a 'night-break' light pulse (Figure 1). The time of maximum repression (NBmax) was completely determined by the time of the transfer to darkness, as other authors have shown (Lumsden *et al*, 1995; Thomas and Vince-Prue, 1997 and references therein). However, the peak times of output rhythms that peak in the day, such as transpiration rate and *LHCB* RNA levels, were little affected by the transition to darkness (Figure 1), instead retaining a similar peak time relative to the start of the light interval. We refer to these contrasting patterns as 'dusk-dominant' and 'dawn-dominant' entrainment, because these terms describe a broader range of behaviour than the fixed-phase relationship implied by dawn or dusk 'tracking'. The question remained whether the clocks in other plants showed similarly flexible control of rhythmic processes.

Entrainment patterns of clock gene RNAs in Arabidopsis

To test this, the timing of clock gene expression was measured under various photoperiods in Arabidopsis, using quantitative PCR (Q-PCR) assays or reporter gene imaging *in vivo*. Figure 2 shows the accumulation of RNA transcripts for three clock genes during photoperiods between 3 and 18 h, followed by constant light (LL) or darkness (DD). The RNA expression profiles were generally advanced to earlier times during the shorter photoperiod treatments, though the detailed photoperiod dependence of the expression profiles varied among the RNAs. The rising portion of the *CCA1* RNA profile at Zeitgeber Time (ZT, where ZT0h=dawn) 16–24 h appears earlier in shorter photoperiods. The timing of the increase changes by only 5 h, comparing 6–18 h photoperiods. The effect appears to be more striking due to the higher peak level of expression in shorter photoperiods (Figure 2A). *CCA1* levels peaked at ZT20–24h; 18-h photoperiods caused a delay of about 4 h compared with 3-h photoperiods. The *TOC1* profile had a broader peak, which is discussed below. The tendency for

increased peak expression under shorter photoperiods was shared to different extents by *TOC1* and *GI* RNAs. Peak *GI* expression moved from ZT6h under 6-h photoperiods to ZT8h under 9- and 12-h photoperiods, and to 8–10 h under 18-h photoperiods (8–10 and 32–34 h in Figure 2C). The 3-h photoperiod caused an unexpected, biphasic profile in *GI*. *GI* RNA peaked in the light at ZT2h (2 and 26 h are replicate time points, Figure 2C) and again in darkness at 6–8 h or in light at 30–32 h (Figure 2C; see Supplementary information).

Phase plane plots of the first cycle of 6-, 12- and 18-h photoperiod data showed the dynamic relationships among the genes more clearly (Supplementary Figure 2), supporting the proposed causal interactions but also highlighting potential exceptions. The shoulder of *TOC1* RNA abundance at ZT16h–20h in the 6-h photoperiod, for example, survived higher expression of its repressor *CCA1* than under longer photoperiods (Supplementary Figure 2C).

RNA expression can be directly regulated by light signalling during the light:dark cycles, which complicates interpretation of the profiles. Circadian regulation is revealed under constant conditions, in LL or DD, where the effects of the entraining light:dark cycles on the clock can be assessed. The times of dusk in the entraining cycles varied by 15 h. In contrast, the peak times of *CCA1* and *GI* RNA fell within a 2–3-h time range in the subsequent cycle in LL (44–68 h in Figure 2A and C). The peak times for each RNA spanned a 4-h time range in DD (24–48 h in Figure 2B, D, F, I and J, and Supplementary Figure 3). The small range of peak times relative to dawn indicates that the gene expression patterns showed only a limited response to the lights-off signal. Entrainment overall was dawn-dominant, more similar to the transpiration and *LHCB* rhythms in *I. nil* than to the flowering rhythm (Figure 1). Simulations of the two-loop model (Locke *et al*, 2005b) illustrate a contrasting, dusk-dominant entrainment: just shortening the photoperiod from 9 to 3 h was sufficient to cause a 3-h change in the simulated RNA peak times under LL (arrowheads in Figure 2G and H) and longer photoperiods caused even larger changes.

The *TOC1* RNA showed characteristically broad peaks. A maximum at ZT8h was observed under 6-h photoperiods and subsequent LL (8 and 32 h, Figure 2E), although profiles in 3- and 9-h photoperiods suggested broader or later peaks at ZT10–12h. A later feature at ZT16–20h created a shoulder on the falling phase. The 3- and 9-h photoperiods were investigated in separate experiments with triplicate samples at 1-h time resolution over the *TOC1* peak. The *TOC1* RNA maximum occurred at ZT10h in 9-h photoperiods and at ZT11h in 3-h photoperiods (Figure 2I and J). Thus, the peak time was not advanced when the time of dusk advanced in short photoperiods, as it was in the two-loop model (Figure 2H), but was instead slightly delayed, reminiscent of the flexibility expected for the three-loop clock model (Locke *et al*, 2006). A feature at ZT8h and the shoulder at ZT16h were also suggested in these high-resolution time series (as indicated in the figure).

Analysis of entrainment patterns in Arabidopsis clock models

The mathematical models of the Arabidopsis clock have contrasting behaviour in light–dark cycles (Locke *et al*, 2006),
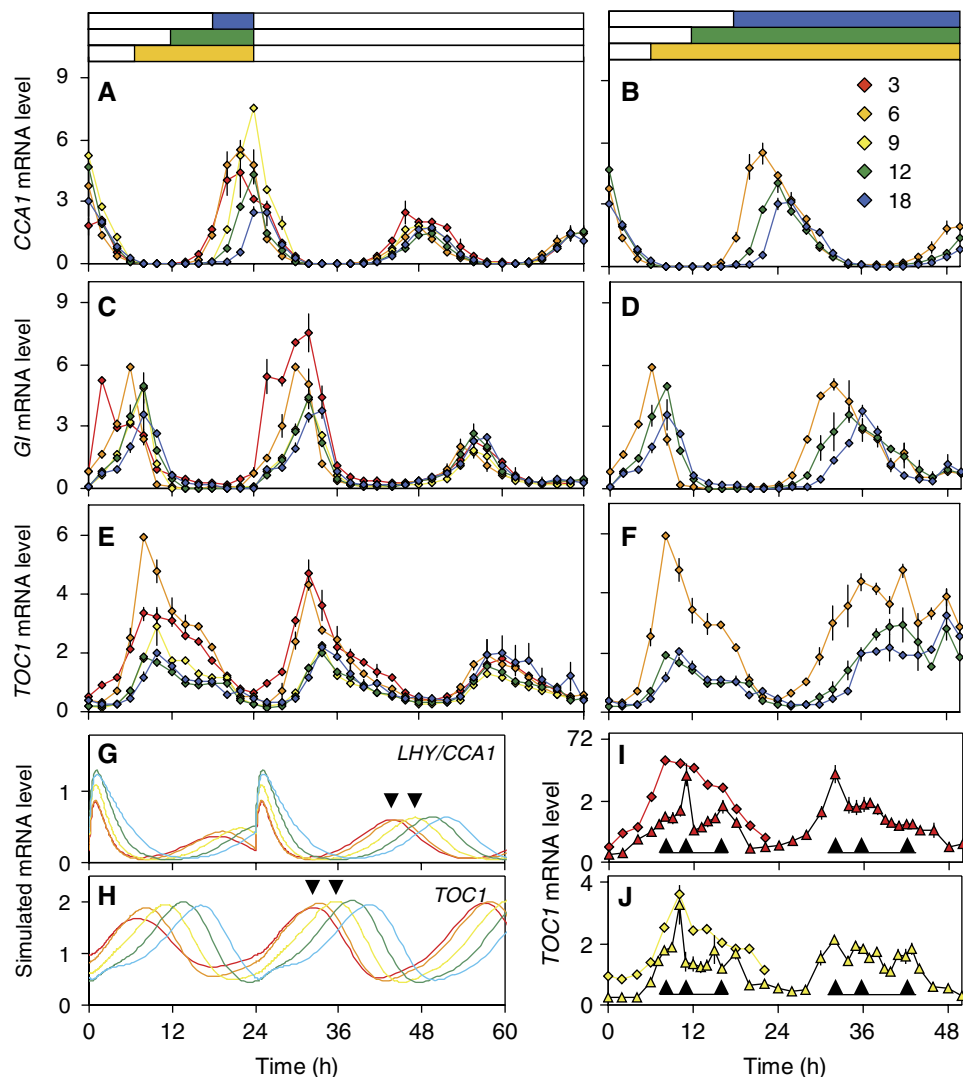
Figure 2 Arabidopsis clock gene expression changes with photoperiod. Transcript abundance measured with 2 h time resolution by Q-PCR relative to an *ACT2* standard, for clock genes *CCA1* (**A**, **B**), *GI* (**C**, **D**) and *TOC1* (**E**, **F**, **I**, **J**) after entrainment to 24-h light:dark cycles (LD), including a photoperiod of 3 h (red), 6 h (orange), 9 h (yellow/black), 12 h (green) or 18 h (blue). Samples were taken during one diurnal cycle and after release into constant light (LL; A, C, E) or darkness (DD; B, D, F). Time-points 0–22 h are identical for LL and DD. Time stamps below (H, J) apply to all panels. Error bars represent the range of biological duplicates (A–F) or the SE of triplicates (I, J). Light conditions for three photoperiods are shown (open bar, light interval; shaded bar, darkness, with colours orange for 6 h photoperiod, green for 12 h, blue for 18 h). Simulations of *LHY* (**G**) and *TOC1* (**H**) RNA levels in the interlocking-loop model illustrate the large phase changes predicted by a dusk-responsive model under this range of photoperiods (3 h, red; 6 h, orange; 9 h, broader yellow; 12 h, green; 15 h, blue). Arrowheads in (G, H) highlight the 3-h phase shift between 3- and 9-h photoperiods. Time series for *TOC1* expression in the 3-h (I) and 9-h (J) photoperiod followed by DD are shown with 1 h time resolution at the peaks, together with equivalent data replotted from (F). Arrowheads in (I, J) mark the complex peak waveform observed in the samples with higher time resolution. Source data is available for this figure at www.nature.com/msb.

and the underlying mechanisms are well defined. We therefore sought to understand the experimental data by comparison with the models. Timing rather than expression level was our focus. Expression levels in the models are arbitrary, because the data available during model construction had not allowed us to constrain the simulated expression levels. Time series from numerical simulation were analysed to find the time at which the simulated RNA levels (shown in full in Supplementary Figure 4) of each clock component reached their peak level, when the model was stably entrained to light–dark cycles (Figure 3B, D and F). The peak times showed contrasting patterns of entrainment for the RNAs (see below).

To show the entrainment patterns for both RNA and protein components in a compact form, we used dynamical systems perturbation theory to develop a measure of dusk sensitivity. The measure reflects how closely the peak and trough times match a *change* in the time of dusk, and is applicable to any entrained oscillator (see Supplementary information). A dusk sensitivity of 1 indicates that the clock component will perfectly track the time of dusk (strongly dusk-dominant entrainment), whereas a component with 0 dusk sensitivity will perfectly track dawn (strongly dawn-dominant entrainment). The measure is intended to follow naturally from the plots of Figure 3B, D and F, where the line joining data points for a dusk-tracking component
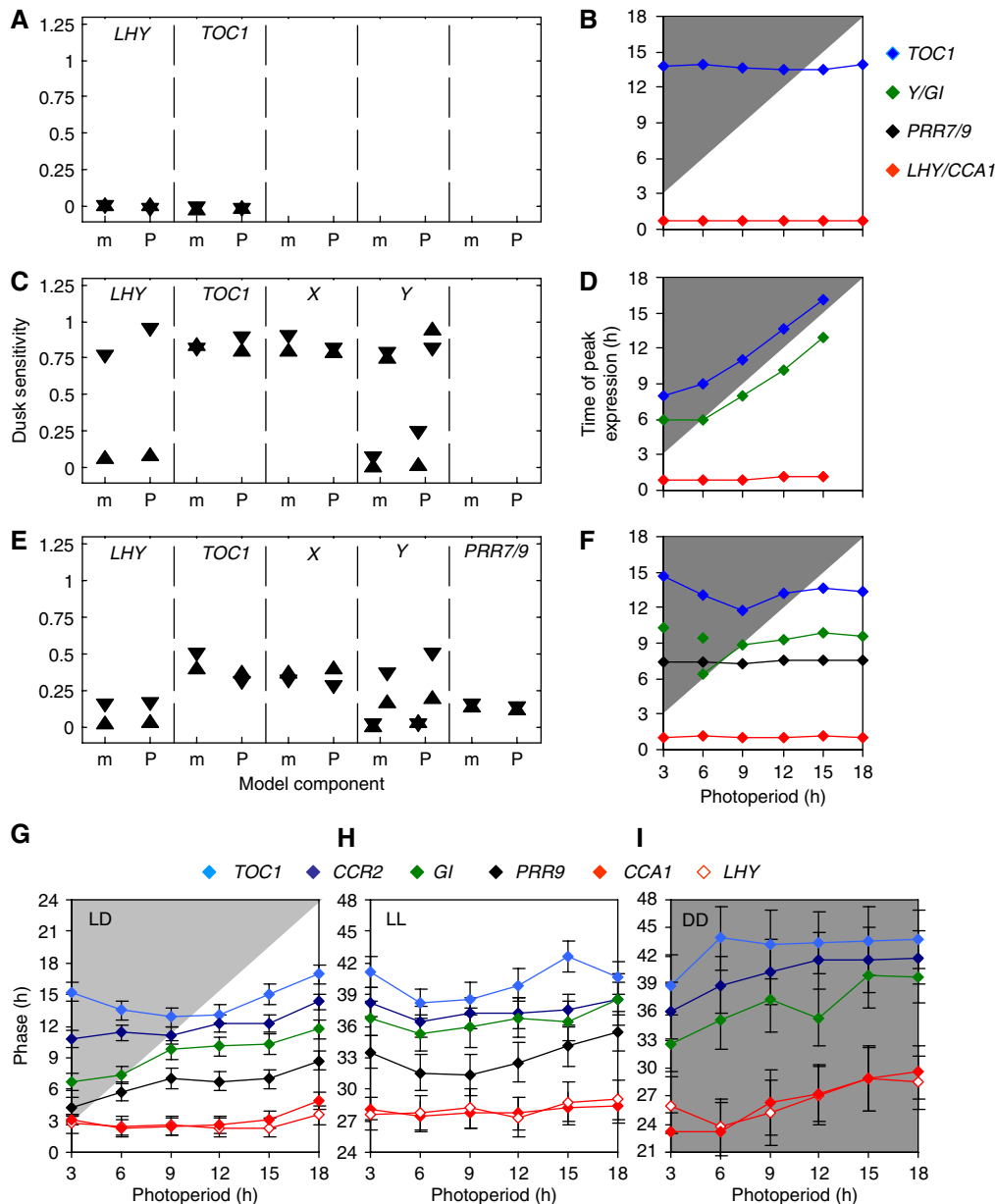
Figure 3 Predicted and experimentally measured entrainment patterns in the clock of Arabidopsis. The one-loop (**A**, **B**), two-loop (**C**, **D**) and three-loop (**E**, **F**) models of the Arabidopsis clock were analysed to calculate the dusk sensitivity measure (A, C, E) for the peak (upward triangle) and trough (downward triangle) times of mRNA (m) and bulk protein (P) variables of all the genes in the model under a 12-h photoperiod. Dusk sensitivity close to 1 indicates dusk-dominant entrainment; close to 0, dawn-dominant entrainment. Where an expression profile has multiple peaks or troughs, its dusk sensitivity is plotted from left to right, in chronological order after dawn, with the convention that in each peak/trough pair the trough follows the peak in time. The models were solved numerically under a range of simulated photoperiods, resulting in the simulated RNA profiles plotted in Supplementary Figure 3. Times of the peak abundance for each simulated RNA during light:dark cycles are shown (B, D, F; see inset key for gene identity). For comparison, the peak expression time for six clock genes was measured in individual seedlings using mFourfit analysis of *in vivo* imaging data (Supplementary Figures 5 and 7) from transgenic plants carrying *LUC* reporter fusions under the same range of photoperiods (**G**), or following transfer to LL (**H**) or DD (**I**; see the inset key for gene identity). *PRR9* is absent from I, because very low expression levels in DD prevented phase estimation. Shaded chart areas represent darkness. Error bars indicate the standard error of the mean, calculated as described in the Supplementary information. Two-way ANOVA on LD, LL and DD peak times showed a highly significant interaction between gene and photoperiod in each case ($P \ll 0.001$), indicating that the genes responded to photoperiod in significantly different patterns. Source data is available for this figure at www.nature.com/msb.

has a gradient of 1, and for a dawn-tracking component has a gradient of 0.

Dusk sensitivity was computed for both peak and trough phases of each clock component for clock models with varying complexity under 12-h photoperiods (Figure 3A, C and E), and

for comparison under 6- and 18-h photoperiods (Supplementary Figure 5). Where a component had multiple peaks or troughs per cycle, their dusk sensitivity was computed separately. The one-loop model (Locke *et al*, 2005a) has light input only to the morning component *LHY/CCA1*

(Supplementary Figure 1), and, in accord with theoretical predictions, entrainment of the whole model is locked to dawn (Figure 3A and B). In the two-loop model (Locke *et al*, 2005b), additional light input via *Y* in the evening loop allowed dusk-dominant entrainment for all components (Figure 3C and D). Only the acute, light-induced peaks of *LHY/CCA1* and *Y* expression after dawn were dawn-dominant (Supplementary Figure 4B and G, and Supplementary information). Neither model changed its behaviour across the range of photoperiod (Supplementary Figure 5A, C and E, and data not shown).

The three-loop model includes an additional feedback loop with light input to *PRR7/9* (Supplementary Figure 1C), which conferred strong dawn dominance to *LHY/CCA1* and *PRR7/9* components (Figure 3E and F). However, the evening loop components *Y* and *TOC1* showed intermediate dusk sensitivity values, indicating more flexible regulation that responded to both signals in the 12-h photoperiod (Figure 3E). This behaviour was altered substantially under the 6- and 18-h photoperiods (Supplementary Figures 5B, D and F), leading us to investigate its mechanisms.

Expression of *Y* showed the light-induced peak at dawn in the three-loop model, followed by a circadian peak at ZT10h (Supplementary Figure 4H), which showed intermediate dusk sensitivity in the 12-h photoperiod (Figure 3E). Under 6- or 9-h photoperiods, lights-off occurred during this peak of *Y* expression (marked in Supplementary Figure 4H). The abrupt end of light-activated transcription curtailed the peak earlier under 6-h than under 9-h photoperiods (Figure 3F), leading to high dusk sensitivity (Supplementary Figure 5B). Under 15- and 18-h photoperiods, *Y* expression was ended by negative feedback from TOC1 in the model's evening loop. This occurred fully within the light interval, so the timing of this peak was unaffected by lights-off (Figure 3F) and its dusk sensitivity was very low (Supplementary Figure 5F).

Simulated *TOC1* RNA lacks direct light regulation in the three-loop model, but its peak time showed a complex response, advancing under 3–9-h photoperiods, then delaying in 15-h photoperiods (Figure 3F). Dusk sensitivity of the simulated *TOC1* peak was negative in short photoperiods, reflecting the fact that the peak occurred earlier in response to later dusk (Supplementary Figure 5B). Simulations of the three-loop model (data not shown) confirmed the intuition that extended light activation of *Y* transcription, which indirectly activates *TOC1* (Supplementary Figure 1C), was responsible for the faster rise in *TOC1* expression in photoperiods up to 9 h (Supplementary Figure 4F), leading to the earlier peak times (Figure 3F and G). Photoperiods greater than 9 h prolonged the light input to *Y*, allowing later *TOC1* peak times, until negative feedback from TOC1 protein in the evening loop repressed *Y* (data not shown). Consistent with these dusk-independent events, dusk sensitivity of the TOC1 peak was low under long photoperiods (Supplementary Figure 5F).

The three-loop model supported flexible entrainment, as the peak times of the clock components changed relative to each other in a photoperiod-dependent manner. None of the components was dusk-sensitive in all photoperiods, in contrast to the two-loop model. Testing the subtle changes in regulation predicted by the model required peak time estimates with higher resolution than our RNA data.

Testing model predictions with *in vivo* reporter gene assays

Clock gene expression was therefore measured using *in vivo* LUCIFERASE (*LUC*) imaging, which avoided the biological variation introduced by sampling different plants at each time point for RNA assays. A modified analytical method, mFourfit, was developed to measure the times of peak expression in entrained rhythms with complex waveforms (see Supplementary information). The longitudinal LUC data allow direct measures of the time of peak expression in individual plants, and the mean and variation of timing in a population, which is the relevant behaviour. The destructive RNA assays, in contrast, reflect the peak time of the average expression level in the population samples but do not allow direct measures of timing. Peak expression times were measured under light:dark cycles (LD) with photoperiods from 3 to 18 h, or following release into LL or DD (Figure 3G–I). The patterns of *LUC* expression (Supplementary Figures 6 and 8) closely followed the cognate mRNA profiles (see Supplementary information). The patterns of *TOC1* timing *in vivo* showed strong similarity to the predictions of the three-loop model (Figure 3G–I). In particular, the *TOC1* reporter showed the earliest peak in 9-h photoperiods (Figure 3G), as predicted by this model (Figure 3F). The peak time in 3-h photoperiods was slightly delayed, consistent with RNA data (Figure 2). *GI* reporter activity showed a dusk-dominant peak in photoperiods up to 9 h, as predicted by the dusk peak of *Y* in the three-loop model (Figure 3F). The *GI* reporter peak time was delayed in photoperiods greater than 9 h, again as predicted. The three-loop model closely reflected the observed regulation of these evening-expressed genes.

The major peaks of *LHY* and *CCA1* expression followed closely after dawn (Figure 3G), as the *LHY/CCA1* peak does in the three-loop model (Figure 3F). These *LUC* reporter profiles also showed an increase in expression before dawn (ZT19h–24h), consistent with the RNA data for *CCA1* (Figure 2A). The observed timing of this initial rise was altered by 3 h in the 6-h photoperiod relative to the 12-h photoperiod conditions, in both RNA and *LUC* data. This indicated greater dusk sensitivity than predicted by the three-loop model, but less than the 5-h change predicted by the two-loop model (Figure 2G; see also Supplementary Figures 4B and C). The *PRR9* reporter's peak time was dawn-dominant (Figure 3G), but less so than the combined *PRR9/7* gene in the three-loop model, which tracked the time of dawn (Figure 3F).

Expression profiles after release into constant light (LL) or constant darkness (DD) more clearly separated the effects of dawn and dusk (Figure 3H and I). Peak times of *LUC* expression were more variable among individual plants than during light:dark cycles. The rise of *CCA1* and *LHY* before dawn formed a distinct peak in short photoperiods under LD, for example, in both RNA data (Figure 2A) and *LUC* profiles (Supplementary Figures 6 and 8). The DD data showed this feature under longer photoperiods, without the intervening light response at dawn. The peak in DD retained dusk sensitivity of about 0.4 in photoperiods from 6 to 18 h ($\sim$5-h delay under a 12-h change in the time of dusk; Figure 3I). The strong resetting effect of dawn was revealed by comparison with the data under LL (Figure 3H), where the peak in *CCA1*

and *LHY* around 27 h reflected the phase set by the previous dawn at 0 h. The dusk sensitivity of this peak in LL was therefore close to 0.

Though the expression profiles were generally more dawn-dominant after release into LL and more dusk-dominant in DD, there was significant variation among genes. The profiles other than *LHY* and *CCA1* showed the earliest peak times in LL after 6–9 h photoperiods (Figure 3H). Thus, their phase was not determined exclusively by dawn-dominant *LHY* and *CCA1*, but was instead reminiscent of the flexible regulation of *TOC1* in LD. In DD, the entrainment pattern of all the genes was more similar to *LHY* and *CCA1*.

Dusk controls evening gene expression in Arabidopsis

None of the core clock genes tested showed the strong dusk dominance across all photoperiods in LD, which had been clear in the flowering rhythm of *I. nil* (Figure 1). We therefore measured RNA expression profiles under 6-, 12- and 18-h photoperiods (Figure 4 and Supplementary Figure 9), for clock-controlled genes involved in biological processes that are known to respond to the lights-off signal, namely the mobilisation of starch reserves (genes STARCH EXCESS 4 (SEX4) and DISPROPORTIONATING ENZYME 2 (DPE2); Chia *et al*, 2004; Niittyla *et al*, 2006) and the photoperiodic control of flowering (genes FLAVIN BINDING KELCH REPEAT 1 (FKF1) and CONSTANS (CO); Imaizumi and Kay, 2006). *CO*, *SEX4* and *DPE2* showed broad expression profiles that hampered the estimation of peak expression time. The half-maximum points of the rising and falling phases were more reliable phase markers (Figure 4A), and have been used in several other circadian studies (Khalsa *et al*, 1992; Roenneberg *et al*, 2005). The *CCA1* RNA rising-phase marker was advanced in 6-h compared with 12-h photoperiods, reflecting the dusk-responsive rise discussed above. The falling-phase marker was dawn-dominant, as expected after resetting at dawn. *GI* and *FKF1* showed a small delay in rising (~2 h) and falling phases (~2–3.5 h) in the 18-h relative to the 6-h photoperiod conditions (Figure 4A), consistent with previous reports (Fowler *et al*, 1999; Imaizumi *et al*, 2003). The rising phase of *CO*, *SEX4* and *DPE2* was more dawn-dominant than their falling phase, which was strongly dusk-dominant (Figure 4B). Light signals were important for *DPE2* and *SEX4* profiles in LD, because both genes showed noisy peaks in LL and very low expression in DD that hampered detailed interpretation of timing. Both genes had previously been scored as rhythmic in LL (Edwards *et al*, 2006; Covington *et al*, 2008; Michael *et al*, 2008), but the clearly dusk-dominant fall in expression was only observed in LD, suggesting that this was a direct light response (Supplementary Figure 9). Timing of *FKF1* and *CO* expression was more dawn dominant in LL than in LD (Supplementary Figure 9), suggesting that the time of lights-off had influenced the *FKF1* and *CO* profiles under LD. The first rise of *FKF1* and *CO* in DD also retained clear dusk responsiveness, suggesting that these genes, especially *CO*, were controlled by a circadian rhythm with dusk-responsive entrainment (Supplementary Figure 9).
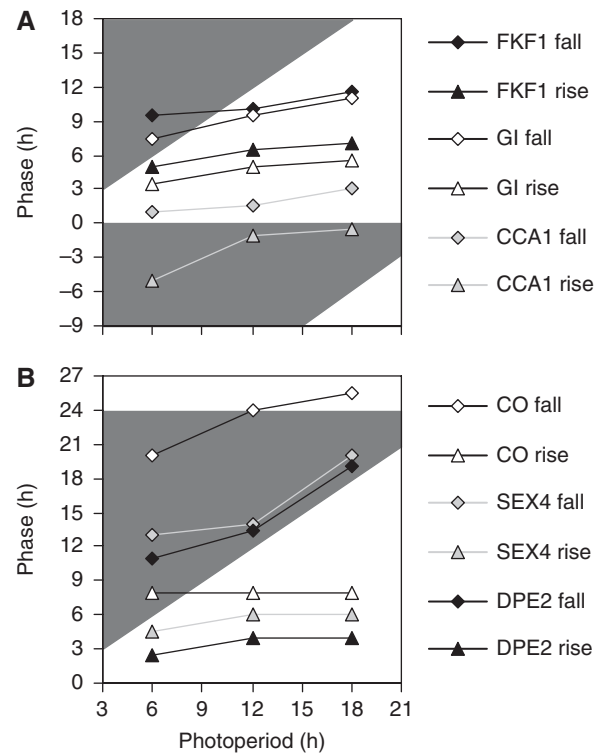
Figure 4 Dawn- and dusk-dominant regulation of Arabidopsis gene expression. RNA abundance of *Arabidopsis* clock genes and clock-controlled genes were measured by Q-PCR data under light:dark cycles with photoperiods of 6, 12 and 18 h (see Figure 2, Supplementary Figure 8). Times of the half-maximum rising (triangles) and falling (diamonds) phases are shown in (**A**) for *CCA1*, *GI* and *FKF1*, and in (**B**) for *CO*, *SEX4* and *DPE2*. See inset keys for gene identification. Shaded areas of plots represent darkness, and open areas, light. Source data is available for this figure at www.nature.com/msb.

Mathematical analysis of processes that control dusk sensitivity

The dusk sensitivity of circadian entrainment determines how clock-controlled genes will change their expression over the seasons. Designing a specific manipulation to the pattern of entrainment is non-trivial, because the pattern is an emergent property of the complex circadian system and all its light inputs. We therefore extended the dusk sensitivity measure to predict which biochemical processes could produce a desired change in the entrainment pattern of any component in the model, using the novel mathematical analysis described in the Supplementary information. As a test case, we sought manipulations that would alter the dusk sensitivity of the three-loop model under a 14-h photoperiod, because this is the condition when feedback in the evening loop limits the dusk sensitivity of the peak in *TOC1* RNA (as discussed above). Processes in the evening loop, including light input to *Y*, were intuitively expected to affect the model's dusk sensitivity, but none was as effective as the transcription of *PRR7/9* (Supplementary Figure 11). This morning loop component represses *LHY/CCA1*, thereby indirectly activating both *Y* and *TOC1* (Supplementary Figure 1C). Simulating a modification of *PRR7/9* transcription in the three-loop model validated the analytical prediction: several clock components were converted from dawn to dusk dominance, including the time of

peak *TOC1* RNA expression (Supplementary Figure 12). The extended analysis can thus prioritise the targets for future experimental investigation.

Discussion

By testing three mathematical models of the Arabidopsis clock, we showed that increased model complexity allowed the circadian phase of the model components to change flexibly in response to the photoperiod of the entraining LD cycle. The morning and evening feedback loops in the three-loop model, in particular, allowed for variation in the phase relationship between the different loops, enabling dawn- and dusk-dominant entrainment within a single gene network. Dusk dominance of the evening genes was predicted only for photoperiods between 6 and 12 h (Figure 3F), but this photoperiod range is physiologically relevant for Arabidopsis (Wilczek *et al*, 2009). This result is analogous to the observed dawn- and dusk-dominant entrainment of the morning and evening oscillators in neural clocks (Jagota *et al*, 2000; Stoleru *et al*, 2004; Inagaki *et al*, 2007). It illustrates the broader principle that multiple feedback loops can increase the flexibility of oscillator models (Rand *et al*, 2004, 2006). The same principle likely applies more generally to the complexity observed in non-oscillatory biological regulators: testing this hypothesis will required suitable mathematical models combined with experiments that manipulate relevant parameters, like the photoperiod variation tested here.

The three-loop model predicted much of the regulatory behaviour that we observed in gene expression data *in vivo*, although the model was constructed only using data for 12-h photoperiods and constant darkness (Locke *et al*, 2006). Dusk-dominant behaviour of the evening genes was observed over the predicted photoperiod range (Figures 2 and 3). The circuit's flexibility was most evident in short photoperiods (<9 h; Figure 3F and G), where the peak of *GI* expression tracked dusk, the peaks of *CCA1* and *LHY* expression were locked to dawn, and the *TOC1* peak time moved slightly later as the time of dusk moved earlier. This response of *TOC1* had not been identified before, as previous studies did not test very short photoperiods (Perales and Mas, 2007; Michael *et al*, 2008). The model's correct and comprehensible prediction for the evening genes indicates the benefits of mathematical modelling in experimental design, and in understanding the interacting factors that control dynamic gene networks.

The model's behaviour can be conceptually divided into the effects of light inputs, the day-time effects of the morning loop upon the evening-expressed genes, and the night-time effects of the evening loop upon the morning-expressed genes. The match to data indicated that the three-loop model recapitulated the day-time effects more accurately than the night-time effects. In particular, the *GI* and *TOC1* data validated the location of light input to *GI* and the circuit structure of the model's evening feedback loop. It does not necessarily follow that the GI and TOC1 proteins are the sole biochemical constituents of the equivalent functions *in vivo* (Locke *et al*, 2006; Martin-Tryon *et al*, 2007; Ito *et al*, 2009). We have previously argued that *GI* cannot constitute all of the *Y* function, for example (Locke *et al*, 2006). The light input at

dawn dominated the behaviour of the morning loop components in the three-loop model, *LHY/CCA1* and *PRR9/7*, whereas the data showed a significant dusk responsiveness in the regulation of *LHY* and *CCA1* before dawn. This must reflect the functions of their regulator(s), represented by the activator *X* and/or the inhibitor *PRR9/7* in the models. *TCP21* (*CHE*) might contribute to this effect for *CCA1* (Pruneda-Paz *et al*, 2009), but its mutant phenotype indicates that it alone is not *X*. The contribution of *PRR9/7* to this effect will be re-evaluated elsewhere, in the light of emerging data.

The observed timing of the clock components was almost always more dawn dominant than dusk dominant, consistent with a strong resetting effect of dawn. Light induction of *LHY/CCA1* at dawn is an important effect of light in the model, and also strongly affects the evening clock components. Light induction of *LHY* and *CCA1* was detectable using the *LUC* reporters (Supplementary information and Supplementary Figure 6). Light induction of *CCA1* and to a lesser extent *LHY* was directly demonstrated by RNA assays at high time resolution (Supplementary Figure 7), despite the light-induced destabilisation of the *CCA1* RNA (Figure 2; Yakir *et al*, 2007). Our data allow direct comparison of the peak levels and rhythmic amplitudes of the clock genes on a broad scale (see Supplementary information), which have been little studied in any system. As many mechanisms affect absolute levels or amplitudes, we focussed on comparisons of timing, usually within a particular data type.

The clock genes provide markers for the core patterns of rhythmic regulation that are available to control thousands of circadian target genes. Under light–dark cycles, rhythmic transcripts detected by microarray assays showed peak times with two significant clusters, around dawn and around dusk (Michael *et al*, 2008). Comparing peak times on a gene-by-gene basis showed that many genes that were expressed up until dusk under 8- or 12-h photoperiods had later peak times under 16-h photoperiods or constant light (Figure 6B and D of Michael *et al*, 2008). This might appear paradoxical, given the absence of dusk-dominant profiles in the clock components. However, direct light signalling and indirect light effects via photosynthetic metabolism are important regulators during light:dark cycles (Blasing *et al*, 2005; Usadel *et al*, 2008). Transcriptome profiles under constant light showed a more even spread of peak times (Harmer *et al*, 2000), though two preferred phases were noted (Edwards *et al*, 2006; Covington *et al*, 2008; Michael *et al*, 2008). The evening-peaking pattern in the array data in LD is consistent with the regulation of evening genes such as *SEX4* and *DPE2* in our data, where each day's light input sets the gene's particular profile and especially its falling phase (Figure 4B and Supplementary Figure 9). Such evening-expressed genes will show dusk-tracking peak times in LD, but this cannot be taken as evidence for a dusk-tracking clock, even if the same genes show *bona fide* circadian regulation in LL. In 6–9-h photoperiods, for example, peak expression of *GI* tracks dusk in our data, as does *Y* in the three-loop model. This reflects light regulation superimposed on a circadian rhythm (Fowler *et al*, 1999).

As the clock controls the plant's responsiveness to light (Millar and Kay, 1996) and temperature (Fowler *et al*, 2005; Dodd *et al*, 2006) signals, the key function of the clock may be to balance direct and indirect environmental inputs to

coordinate physiological and metabolic functions. Correct timing of rhythmic processes such as starch degradation is crucial for growth (Graf *et al*, 2010), so it is very likely that this temporal regulation of vegetative physiology has been subject to natural selection, and might contribute to crop improvement. Dusk sensitivity (Figure 3) and similar tools for targeted mathematical analysis of complex biological models help not only to understand the interacting genetic factors that contribute to temporal regulation, but also to prioritise the targets for manipulation (Supplementary Figures 11 and 12).

Natural genetic variation provides evidence (Bohlenius *et al*, 2006) of selection acting upon the dusk-dominant, photoperiod response rhythm in short-day plants (Figure 1). Strongly dusk-dominant rhythms seem less important for most gene expression profiles in Arabidopsis than the termination of light induction at dusk. However, the short-day species themselves show several dawn-dominant rhythms in gene expression and in processes involved in vegetative growth (Figure 1; Hayama *et al*, 2007). Conversely, the Arabidopsis photoperiod sensor gene *CO* showed an unusual degree of dusk-dominant, circadian control, apparently greater than its functional partner *FKF1* (Figure 4B and Supplementary Figure 9). Additional mechanisms, such as further feedback loops, might of course affect the timing of specific genes in all cells. Alternatively, a cell-type-specific circadian clock that is modified for dusk dominance might exist in the phloem companion cells that express *CO* (An *et al*, 2004), without detectably affecting the results for other genes tested, because our assays averaged across all cells. Evidence for tissue-specific, and in particular vascular-specific, timing has been provided (Thain *et al*, 2002; Fukuda *et al*, 2007; Para *et al*, 2007; James *et al*, 2008). Differentiated regulation of the circadian clock might thus contribute to cell-type-specific processes, such as the photoperiod sensor, adding to the complexity of feedback loops within each cell.

Materials and methods

Plant materials and growth conditions

Seeds of *I. nil* (*Pharbitis nil*) Choisy cv. Violet were planted and grown as described (Lumsden *et al*, 1995). Unless otherwise noted, all Arabidopsis seeds were sterilised and grown on solid media containing 3% sucrose, as described previously (Edwards *et al*, 2005). Seedlings for *Luciferase* imaging were grown for 4 days at 22°C in Sanyo MLR350 environmental test chambers (Sanyo, Osaka, Japan) under experimental photoperiods of 75 µmol m^{-2} s^{-1} cool white fluorescent light. Seedlings were then transferred to Percival I-30BLL growth chambers (CLF Plant Climatics, Emersacker, Germany) at dawn on the 5th day and grown at 22°C under an equal mix of Red and Blue LEDs at 20–30 µmol m^{-2} s^{-1}. *CCA1:LUC+*, *CCR2:LUC+*, *LHY:LUC+* and *TOC1:LUC+* plants have been described (Doyle *et al*, 2002; McWatters *et al*, 2007). See Supplementary information for details on construction of *GI:LUC+*, *PRR9:LUC+* and *35S:LUC+* lines. For Q-PCR experiments, wild-type Wassilewskija seedlings were grown for 7 days in Percival growth chambers under experimental photoperiods of 60–65 µmol m^{-2} s^{-1} cool white fluorescent light.

Measurement of photoperiodic response in *I. nil*

The method was essentially as described (Lumsden *et al*, 1995). Seedlings were grown in continuous light, and, after durations of between 72 and 96 h, 'released' into a dark period of 48 h. During the first 12 h of darkness, night breaks of 10 min red light were given at hourly intervals, to determine the time of maximal response to the night break. This time is termed NBmax.

Transpiration rate measurement

Plants of *I. nil* were grown as described above, and the mass of individual plants was recorded using a computerised system, to yield a time-series record of weight loss due to transpiration. The plant + pot was weighed using Precisa 125A balances (Milton Keynes, UK) with automatic output via an RS232 port to an IBM PC-compatible computer. The system recorded the weight of each plant at 10-min intervals, from up to six balances in each experiment. Each recorded value is the mean of 10 individual measurements.

Measurement of gene expression

For RNA measurements in *I. nil*, plants were grown as described above. Total RNA was isolated as described (Kolar *et al*, 1995). The abundance of CAB (=*LHCB*) transcripts was determined on RNA gel blots using 20 µg of total RNA per sample, and hybridised to a radio-labelled tomato LHCII type1 *CAB1* probe as described (Kolar *et al*, 1995).

For quantitative RT–PCR in Arabidopsis, seedlings were harvested, and RNA was extracted and reverse transcribed as described previously (Locke *et al*, 2005b). Q-PCR was carried out using SYBR Green JumpStart *Taq* ReadyMix (Sigma, Gillingham, UK) in technical triplicate using the Relative Quantification function of a Light Cycler 480 (Roche, UK) to measure mRNA abundance. Expression values were normalised against *ACTIN 2* (*ACT2*). *ACT2*, *TOC1*, *CCA1*, *LHY* and *GI* primers have previously been described (Locke *et al*, 2005b; Edwards *et al*, 2006). See Supplementary information for other Q-PCR primer sequences.

Luciferase imaging was carried out as previously described (Gould *et al*, 2006) using Hamamatsu C4742-98 digital cameras operating at −75°C under control of Wasabi software (Hamamatsu Photonics, Hamamatsu City, Japan). Imaging was started at dawn on the 6th day of growth. Bioluminescence levels were quantified using Metamorph software (MDS, Toronto, Canada) and phase estimates were produced with the mFourfit function of BRASSv3 (Locke *et al*, 2005b; available at http://www.amillar.org; see Supplementary information). Each experiment included 22 individual seedlings of each genotype; experiments were replicated seven or more times per photoperiod for LD (four or more experiments released into LL conditions, and three or more into DD).

Model simulation and analysis

Model simulations were carried out on the published models and parameter sets (Locke *et al*, 2005a, b, 2006) using the Circadian Modelling interface (available from http://www.amillar.org). Simulations were entrained for 20 days under the respective photoperiods and then released into LL or DD for 10 days. Details of the dusk sensitivity analyses are given in the Supplementary information.

Supplementary information

Supplementary information is available at the *Molecular Systems Biology* website (http://www.nature.com/msb).

implemented data analysis; KDE and AWT performed data analysis; KDE, AP and OEA performed model simulations; OEA designed and performed model analysis; KDE, OEA and AJM wrote the paper.

Conflict of interest

The authors declare that they have no conflict of interest.

References

Akman OE, Rand DA, Brown PE, Millar AJ (2010) Robustness from flexibility in the fungal circadian clock. *BMC Syst Biol* **4:** 88

An H, Roussot C, Suarez-Lopez P, Corbesier L, Vincent C, Pineiro M, Hepworth S, Mouradov A, Justin S, Turnbull C, Coupland G (2004) CONSTANS acts in the phloem to regulate a systemic signal that induces photoperiodic flowering of Arabidopsis. *Development* **131:** 3615–3626

Bell-Pedersen D, Cassone VM, Earnest DJ, Golden SS, Hardin PE, Thomas TL, Zoran MJ (2005) Circadian rhythms from multiple oscillators: lessons from diverse organisms. *Nat Rev Genet* **6:** 544–556

Blasing OE, Gibon Y, Gunther M, Hohne M, Morcuende R, Osuna D, Thimm O, Usadel B, Scheible WR, Stitt M (2005) Sugars and circadian regulation make major contributions to the global regulation of diurnal gene expression in Arabidopsis. *Plant Cell* **17:** 3257–3281

Bohlenius H, Huang T, Charbonnel-Campaa L, Brunner AM, Jansson S, Strauss SH, Nilsson O (2006) CO/FT regulatory module controls timing of flowering and seasonal growth cessation in trees. *Science* **312:** 1040–1043

Chia T, Thorneycroft D, Chapple A, Messerli G, Chen J, Zeeman SC, Smith SM, Smith AM (2004) A cytosolic glucosyltransferase is required for conversion of starch to sucrose in Arabidopsis leaves at night. *Plant J* **37:** 853–863

Covington MF, Maloof JN, Straume M, Kay SA, Harmer SL (2008) Global transcriptome analysis reveals circadian regulation of key pathways in plant growth and development. *Genome Biol* **9:** R130

Dodd AN, Gardner MJ, Hotta CT, Hubbard KE, Dalchau N, Love J, Assie JM, Robertson FC, Jakobsen MK, Goncalves J, Sanders D, Webb AA (2007) The Arabidopsis circadian clock incorporates a cADPR-based feedback loop. *Science* **318:** 1789–1792

Dodd AN, Jakobsen MK, Baker AJ, Telzerow A, Hou SW, Laplaze L, Barrot L, Poethig RS, Haseloff J, Webb AA (2006) Time of day modulates low-temperature Ca signals in Arabidopsis. *Plant J* **48:** 962–973

Dodd AN, Salathia N, Hall A, Kevei E, Toth R, Nagy F, Hibberd JM, Millar AJ, Webb AA (2005) Plant circadian clocks increase photosynthesis, growth, survival, and competitive advantage. *Science* **309:** 630–633

Doyle MR, Davis SJ, Bastow RM, McWatters HG, Kozma-Bognar L, Nagy F, Millar AJ, Amasino RM (2002) The ELF4 gene controls circadian rhythms and flowering time in *Arabidopsis thaliana*. *Nature* **419:** 74–77

Dunlap JC, Loros JJ, DeCoursey PJ (2004) *Chronobiology: Biological Timekeeping*. Sunderland, MA: Sinauer Associates

Edwards KD, Anderson PE, Hall A, Salathia NS, Locke JC, Lynn JR, Straume M, Smith JQ, Millar AJ (2006) *FLOWERING LOCUS C* mediates natural variation in the high-temperature response of the Arabidopsis circadian clock. *Plant Cell* **18:** 639–650

Edwards KD, Lynn JR, Gyula P, Nagy F, Millar AJ (2005) Natural allelic variation in the temperature-compensation mechanisms of the *Arabidopsis thaliana* circadian clock. *Genetics* **170:** 387–400

Fowler S, Lee K, Onouchi H, Samach A, Richardson K, Coupland G, Putterill J (1999) *GIGANTEA*: a circadian clock-controlled gene that regulates photoperiodic flowering in Arabidopsis and encodes a protein with several possible membrane-spanning domains. *EMBO J* **18:** 4679–4688

Fowler SG, Cook D, Thomashow MF (2005) Low temperature induction of Arabidopsis CBF1, 2, and 3 is gated by the circadian clock. *Plant Physiol* **137:** 961–968

Fukuda H, Nakamichi N, Hisatsune M, Murase H, Mizuno T (2007) Synchronization of plant circadian oscillators with a phase delay effect of the vein network. *Phys Rev Lett* **99:** 098102

Gould PD, Locke JC, Larue C, Southern MM, Davis SJ, Hanano S, Moyle R, Milich R, Putterill J, Millar AJ, Hall A (2006) The molecular basis of temperature compensation in the Arabidopsis circadian clock. *Plant Cell* **18:** 1177–1187

Graf A, Schlereth A, Stitt M, Smith AM (2010) Circadian control of carbohydrate availability for growth in Arabidopsis plants at night. *Proc Natl Acad Sci USA* **107:** 9458–9463

Harmer SL, Hogenesch JB, Straume M, Chang HS, Han B, Zhu T, Wang X, Kreps JA, Kay SA (2000) Orchestrated transcription of key pathways in Arabidopsis by the circadian clock. *Science* **290:** 2110–2113

Hayama R, Agashe B, Luley E, King R, Coupland G (2007) A circadian rhythm set by dusk determines the expression of FT homologs and the short-day photoperiodic flowering response in Pharbitis. *Plant Cell* **19:** 2988–3000

Hazen SP, Schultz TF, Pruneda-Paz JL, Borevitz JO, Ecker JR, Kay SA (2005) LUX ARRHYTHMO encodes a Myb domain protein essential for circadian rhythms. *Proc Natl Acad Sci USA* **102:** 10387–10392

Hazlerigg D, Loudon A (2008) New insights into ancient seasonal life timers. *Curr Biol* **18:** R795–R804

Heide OM, King RW, Evans LT (1988) The semidian rhythm in flowering response of pharbitis-nil in relation to dark period time measurement and to a circadian-rhythm. *Physiol Plant* **73:** 286–294

Imaizumi T, Kay SA (2006) Photoperiodic control of flowering: not only by coincidence. *Trends Plant Sci* **11:** 550–558

Imaizumi T, Tran HG, Swartz TE, Briggs WR, Kay SA (2003) FKF1 is essential for photoperiodic-specific light signalling in Arabidopsis. *Nature* **426:** 302–306

Inagaki N, Honma S, Ono D, Tanahashi Y, Honma K (2007) Separate oscillating cell groups in mouse suprachiasmatic nucleus couple photoperiodically to the onset and end of daily activity. *Proc Natl Acad Sci USA* **104:** 7664–7669

Ito S, Kawamura H, Niwa Y, Nakamichi N, Yamashino T, Mizuno T (2009) A genetic study of the Arabidopsis circadian clock with reference to the TIMING OF CAB EXPRESSION 1 (TOC1) gene. *Plant Cell Physiol* **50:** 290–303

Jagota A, de la Iglesia HO, Schwartz WJ (2000) Morning and evening circadian oscillations in the suprachiasmatic nucleus *in vitro*. *Nat Neurosci* **3:** 372–376

James AB, Monreal JA, Nimmo GA, Kelly CL, Herzyk P, Jenkins GI, Nimmo HG (2008) The circadian clock in Arabidopsis roots is a simplified slave version of the clock in shoots. *Science* **322:** 1832–1835

Khalsa SBS, Whitmore D, Block GD (1992) Stopping the circadian pacemaker with inhibitors of protein synthesis. *Proc Natl Acad Sci USA* **89:** 10862–10866

Kitano H (2007) Towards a theory of biological robustness. *Mol Syst Biol* **3:** 137

Kitayama Y, Nishiwaki T, Terauchi K, Kondo T (2008) Dual KaiC-based oscillations constitute the circadian system of cyanobacteria. *Genes Dev* **22:** 1513–1521

Kolar C, Adam E, Schafer E, Nagy F (1995) Expression of tobacco genes for light-harvesting chlorophyll a/b binding proteins of photosystem II is controlled by two circadian oscillators in a developmentally regulated fashion. *Proc Natl Acad Sci USA* **92:** 2174–2178

Locke JC, Kozma-Bognar L, Gould PD, Feher B, Kevei E, Nagy F, Turner MS, Hall A, Millar AJ (2006) Experimental validation of a predicted feedback loop in the multi-oscillator clock of *Arabidopsis thaliana*. *Mol Syst Biol* **2:** 59

Locke JC, Millar AJ, Turner MS (2005a) Modelling genetic networks with noisy and varied experimental data: the circadian clock in *Arabidopsis thaliana*. *J Theor Biol* **234:** 383–393

Locke JC, Southern MM, Kozma-Bognar L, Hibberd V, Brown PE, Turner MS, Millar AJ (2005b) Extension of a genetic network model

by iterative experimentation and mathematical analysis. *Mol Syst Biol* **1**: 13

Love J, Dodd AN, Webb AA (2004) Circadian and diurnal calcium oscillations encode photoperiodic information in Arabidopsis. *Plant Cell* **16**: 956–966

Lumsden PJ, Youngs JA, Thomas B, Vince-Prue D (1995) Evidence that photoperiodic, dark time measurement in pharbitis-nil involves a circadian rather than a semidian rhythm. *Plant Cell Environ* **18**: 1403–1410

Martin-Tryon EL, Kreps JA, Harmer SL (2007) GIGANTEA acts in blue light signaling and has biochemically separable roles in circadian clock and flowering time regulation. *Plant Physiol* **143**: 473–486

McClung CR (2006) Plant circadian rhythms. *Plant Cell* **18**: 792–803

McWatters HG, Bastow RM, Hall A, Millar AJ (2000) The *ELF3 zeitnehmer* regulates light signalling to the circadian clock. *Nature* **408**: 716–720

McWatters HG, Kolmos E, Hall A, Doyle MR, Amasino RM, Gyula P, Nagy F, Millar AJ, Davis SJ (2007) ELF4 is required for oscillatory properties of the circadian clock. *Plant Physiol* **144**: 391–401

Michael TP, Mockler TC, Breton G, McEntee C, Byer A, Trout JD, Hazen SP, Shen R, Priest HD, Sullivan CM, Givan SA, Yanovsky M, Hong F, Kay SA, Chory J (2008) Network discovery pipeline elucidates conserved time-of-day-specific cis-regulatory modules. *PLoS Genet* **4**: e14

Millar AJ, Kay SA (1996) Integration of circadian and phototransduction pathways in the network controlling CAB gene transcription in Arabidopsis. *Proc Natl Acad Sci USA* **93**: 15491–15496

Niittyla T, Comparot-Moss S, Lue WL, Messerli G, Trevisan M, Seymour MD, Gatehouse JA, Villadsen D, Smith SM, Chen J, Zeeman SC, Smith AM (2006) Similar protein phosphatases control starch metabolism in plants and glycogen metabolism in mammals. *J Biol Chem* **281**: 11815–11818

Ouyang Y, Andersson CR, Kondo T, Golden SS, Johnson CH (1998) Resonating circadian clocks enhance fitness in cyanobacteria. *Proc Natl Acad Sci USA* **95**: 8660–8664

Panda S, Antoch MP, Miller BH, Su AI, Schook AB, Straume M, Schultz PG, Kay SA, Takahashi JS, Hogenesch JB (2002) Coordinated transcription of key pathways in the mouse by the circadian clock. *Cell* **109**: 307–320

Para A, Farre EM, Imaizumi T, Pruneda-Paz JL, Harmon FG, Kay SA (2007) PRR3 Is a vascular regulator of TOC1 stability in the Arabidopsis circadian clock. *Plant Cell* **19**: 3462–3473

Perales M, Mas P (2007) A functional link between rhythmic changes in chromatin structure and the Arabidopsis biological clock. *Plant Cell* **19**: 2111–2123

Pittendrigh CS, Daan S (1976) A functional analysis of circadian pacemakers in nocturnal rodents. V. A clock for all seasons. *J Comp Physiol A* **106**: 333–355

Pruneda-Paz JL, Breton G, Para A, Kay SA (2009) A functional genomics approach reveals CHE as a component of the Arabidopsis circadian clock. *Science* **323**: 1481–1485

Rand DA, Shulgin BV, Salazar D, Millar AJ (2004) Design principles underlying circadian clocks. *J Roy Soc Interface* **1**: 119–130

Rand DA, Shulgin BV, Salazar JD, Millar AJ (2006) Uncovering the design principles of circadian clocks: mathematical analysis of flexibility and evolutionary goals. *J Theor Biol* **238**: 616–635

Roenneberg T, Dragovic Z, Merrow M (2005) Demasking biological oscillators: properties and principles of entrainment exemplified by the Neurospora circadian clock. *Proc Natl Acad Sci USA* **102**: 7742–7747

Smith SM, Fulton DC, Chia T, Thorneycroft D, Chapple A, Dunstan H, Hylton C, Zeeman SC, Smith AM (2004) Diurnal changes in the transcriptome encoding enzymes of starch metabolism provide evidence for both transcriptional and posttranscriptional regulation of starch metabolism in Arabidopsis leaves. *Plant Physiol* **136**: 2687–2699

Stoleru D, Peng Y, Agosto J, Rosbash M (2004) Coupled oscillators control morning and evening locomotor behaviour of *Drosophila*. *Nature* **431**: 862–868

Thain SC, Hall A, Millar AJ (2000) Functional independence of circadian clocks that regulate plant gene expression. *Curr Biol* **10**: 951–956

Thain SC, Murtas G, Lynn JR, McGrath RB, Millar AJ (2002) The circadian clock that controls gene expression in Arabidopsis is tissue specific. *Plant Physiol* **130**: 102–110

Thomas B, Vince-Prue D (1997) *Photoperiodism in Plants*. San Diego, CA: Academic Press

Troein C, Locke JC, Turner MS, Millar AJ (2009) Weather and seasons together demand complex biological clocks. *Curr Biol* **19**: 1961–1964

Tsai TY, Choi YS, Ma W, Pomerening JR, Tang C, Ferrell Jr JE (2008) Robust, tunable biological oscillations from interlinked positive and negative feedback loops. *Science* **321**: 126–129

Ueda HR, Chen W, Adachi A, Wakamatsu H, Hayashi S, Takasugi T, Nagano M, Nakahama K, Suzuki Y, Sugano S, Iino M, Shigeyoshi Y, Hashimoto S (2002) A transcription factor response element for gene expression during circadian night. *Nature* **418**: 534–539

Usadel B, Blasing OE, Gibon Y, Retzlaff K, Hohne M, Gunther M, Stitt M (2008) Global transcript levels respond to small changes of the carbon status during progressive exhaustion of carbohydrates in Arabidopsis Rosettes. *Plant Physiol* **146**: 1834–1861

Wilczek AM, Roe JL, Knapp MC, Cooper MD, Lopez-Gallego C, Martin LJ, Muir CD, Sim S, Walker A, Anderson J, Egan JF, Moyers BT, Petipas R, Giakountis A, Charbit E, Coupland G, Welch SM, Schmitt J (2009) Effects of genetic perturbation on seasonal life history plasticity. *Science* **323**: 930–934

Yakir E, Hilman D, Hassidim M, Green RM (2007) CIRCADIAN CLOCK ASSOCIATED1 transcript stability and the entrainment of the circadian clock in Arabidopsis. *Plant Physiol* **145**: 925–932

Zeeman SC, Smith SM, Smith AM (2007) The diurnal metabolism of leaf starch. *Biochem J* **401**: 13–28

Zeilinger MN, Farre EM, Taylor SR, Kay SA, Doyle III FJ (2006) A novel computational model of the circadian clock in Arabidopsis that incorporates PRR7 and PRR9. *Mol Syst Biol* **2**: 58